

JGR Biogeosciences

RESEARCH ARTICLE

10.1029/2024JG008108

Key Points:

- Both field measured and remotely sensed trait data improved biomass predictions, but only by a small amount
- In the Amazon region, maximum temperature, but not soil fertility, improved biomass predictions
- Trait data was better than structure data for predicting tropical forest net primary production and gross primary production

Supporting Information:

Supporting Information may be found in the online version of this article.

Correspondence to:

C. E. Doughty,
chris.doughty@nau.edu

Citation:

Doughty, C. E., Gaillard, C., Burns, P., Malhi, Y., Shenkin, A., Minor, D., et al. (2024). Satellite derived trait data slightly improves tropical forest biomass, NPP and GPP estimates. *Journal of Geophysical Research: Biogeosciences*, 129, e2024JG008108. <https://doi.org/10.1029/2024JG008108>

Received 27 FEB 2024






Accepted 18 JUN 2024

Author Contributions:

Conceptualization: Christopher E. Doughty, Scott Goetz, Hao Tang
Formal analysis: Christopher E. Doughty
Methodology: Christopher E. Doughty, Patrick Burns, Alexander Shenkin, David Minor, Laura Duncanson, Jesús Aguirre-Gutiérrez
Writing – original draft: Christopher E. Doughty
Writing – review & editing: Camille Gaillard, Laura Duncanson, Jesús Aguirre-Gutiérrez, Scott Goetz, Hao Tang

© 2024. American Geophysical Union. All Rights Reserved.

Satellite Derived Trait Data Slightly Improves Tropical Forest Biomass, NPP and GPP Estimates

Christopher E. Doughty¹ , Camille Gaillard¹, Patrick Burns¹ , Yadvinder Malhi², Alexander Shenkin¹, David Minor³, Laura Duncanson³ , Jesús Aguirre-Gutiérrez² , Scott Goetz¹, and Hao Tang⁴ 

¹School of Informatics, Computing, and Cyber Systems, Northern Arizona University, Flagstaff, AZ, USA, ²Environmental Change Institute, School of Geography and the Environment, University of Oxford, Oxford, UK, ³Geographical Sciences, University of Maryland, College Park, MD, USA, ⁴Department of Geography, National University of Singapore, Singapore, Singapore

Abstract Improving tropical forest current biomass estimates can help more accurately evaluate ecosystem services in tropical forests. The Global Ecosystem Dynamics Investigation (GEDI) lidar provides detailed 3D forest structure and height data, which can be used to improve above-ground biomass estimates. However, there is still debate on how best to predict tropical forest biomass using GEDI data. Here we compare stand biomass predicted by GEDI data with the observed data of 2,102 inventory plots in tropical forests and find that adding a remotely sensed (RS) trait map of leaf mass area (LMA) significantly ($P < 0.001$) improves field biomass predictions, but by only a small amount ($r^2 = 0.01$). However, it may also help reduce the bias of the residuals because there was a negative relationship between both LMA (r^2 of 0.34) and percentage of phosphorus (%P, $r^2 = 0.31$) and residuals. Leaf spectral data (400–1,075 nm) from 523 individual trees along a Peruvian tropical forest elevation gradient predicted Diameter at Breast height (DBH) (the critical measurement underlying plot biomass) with an $r^2 = 0.01$ and LMA predicts DBH with an $r^2 = 0.04$. Other data sets may offer further improvements and max temperature (T_{\max}) predicts Amazonian biomass residuals with an r^2 of 0.76 ($N = 66$). Finally, for a network of net primary production (NPP) and gross primary production (GPP) plots ($N = 21$), leaf traits predicted with remote sensing are better at predicting fluxes than structure variables. Overall, trait maps, especially future improved ones produced by Surface Biology Geology, may improve biomass and carbon flux predictions by a small but significant amount.

Plain Language Summary Improving predictions of tropical forest biomass can help us to fight climate change. In this paper, we tried to improve tropical forest biomass predictions of satellite lidar (Global Ecosystem Dynamics Investigation) by adding remote sensed estimates of leaf traits. Leaf traits like leaf mass area or phosphorus slightly improved predictions of forest biomass with both a ground data set and a remotely sensed data set. Further, remotely sensed trait data could help explain the differences in the prediction of remotely sensed biomass compared with field derived biomass (residuals). Maximum temperature, but not soil fertility, also improved biomass predictions. Remotely sensed leaf traits were better than structure, like tree height, for predicting net primary production (NPP) and gross primary production (GPP). Future improved hyperspectral satellite data may be used to further improve predictions of biomass, NPP and GPP.

1. Introduction

In an era of rapid climate change, accurately predicting forest carbon stocks is increasingly important because carbon stored in forests can potentially offset anthropogenic emissions that cause climate change. For this reason, international climate agreements such as REDD+ (Reducing Emissions from Deforestation and Degradation) have been developed to encourage countries to conserve their forests (Goetz et al., 2015). Using forests as natural climate change solutions, by incentivizing carbon trading and offset schemes, requires accurate and repeatable measurements of forest aboveground biomass (AGB) (Goetz et al., 2015). Earth observation satellite remote sensing (RS), coupled with ground-based measurements, have the potential to provide systematic estimates of AGB over vast spatial extents. Therefore, much effort has been put into developing such maps of AGB, albeit with mixed results. For instance, two remotely sensed biomass maps showed markedly different biomass trends from each other and from 413 ground plots (Avitabile et al., 2016; Baccini et al., 2012; Mitchard et al., 2014; Saatchi et al., 2011). Mitchard et al. (2013, 2014) found the uncertainties were actually >25% more than those listed in the

RS maps of Baccini et al. (2012) and Saatchi et al. (2011) (Mitchard et al., 2013, 2014). They advise to incorporate basal area-weighted wood density estimates and note that depending only on the relationships between tree height and biomass may lead to large, spatially correlated errors. Partially in response to such difficulties in predicting biomass with optical RS, the Global Ecosystem Dynamics Investigation (GEDI) Lidar mission was launched and installed on the International Space Station (ISS) in late 2018 and operational products started in March 2019 (R. Dubayah et al., 2020). GEDI is the first spaceborne lidar designed for terrestrial ecosystem research and the first specifically developed to accurately measure forest canopy 3D structure. However, converting from laser energy returns to accurate biomass predictions is not trivial.

GEDI covers most land areas below 52° latitude, but it does not provide wall to wall coverage and gaps between GEDI tracks are greatest at tropical latitudes owing to the orbital configuration of the ISS (R. Dubayah et al., 2022). To develop pre-launch calibrated models of AGB, ground biomass plots were combined with coincident aircraft lidar data using a waveform simulator (Hancock et al., 2019) to produce the GEDI Level-4A (footprint level) algorithm (Duncanson et al., 2022). Currently the L4A product for tropical forests uses relative height (RH -the height that a certain quantile of energy is returned relative to the ground) 98 and RH 50 to predict a median AGB of 300 Mg Ha⁻¹ for tropical forests (0.66 r^2 and RMSE of 10.4). Duncanson et al. (2022) compares these results to previous studies. For instance, Asner and Mascaró (2014) used a network of 804 field inventory plots and aircraft discrete return lidar in 5 tropical countries to estimate biomass with a $R^2 = 0.92$ and RMSE = 17.1 Mg/ha. Saatchi et al. (2011) combined several data sets with a Maximum Entropy modeling framework across the tropics to get an r^2 of 0.80 and RMSE = 23.8. Baccini et al. (2012) used GLAS (Global Laser Altimetry System) on IceSat-1 together with image data from MODIS (MODerate resolution Imaging Sensor) to estimate biomass across the tropics in a modeling framework of ordinary least squares regression and random forest machine learning algorithms with predictors of HOME (Height of Median Energy), other Height Metrics, and total Canopy returned energy to get an r^2 of 0.83 and RMSE = 22.6. These early studies exemplify the wide variety of techniques and accuracies used to predict biomass in tropical forests. Forest structure data products derived from GEDI are also related to AGB. For instance, Doughty et al. (2023) found forest stratification (% of forests with only one peak in PAVD (Plant Area Volume Density) vs. those with several peaks) correlated with biomass more strongly than tree height (Doughty et al., 2023). Duncanson et al. (2022) used algorithms stratified by 4 plant functional types and 6 world regions but did not include other remotely sensed (e.g., optical image) data as predictor variables for biomass. Here we explore the extent to which incorporating external data sets and having more regional calibrations can improve GEDI biomass predictions across tropical forests.

Environment (e.g., soils and climate) influences the community assembly of tropical forests and knowing species composition could improve biomass estimates since different species have different wood density and structure. For instance, Amazonian plant biogeography may follow a south-west/north-east soil fertility gradient and a north-west/south-east precipitation gradient (ter Steege et al., 2006). Soil cation concentrations are the primary driver of floristic variation for Amazonian trees (Tuomisto et al., 2019) with climate being of secondary importance. However, in central African forests, climate is considered to be the driving factor of floristic patterns (Réjou-Méchain et al., 2021). Therefore, inclusion of soils or forest floristic maps could improve biomass predictions, since both are key variables in different biogeographic zones. Floristics could also determine the relationship between leaf traits and biomass.

Leaf traits may also improve tropical forest biomass predictions. One global study of plant traits found that three-quarters of trait variation is captured in a two-dimensional global spectrum of plant form and function (Díaz et al., 2016). One major dimension within this plane reflects the size of whole plants and their parts; the other represents the leaf economics spectrum, which balances leaf construction costs against growth potential (Díaz et al., 2016). Since the size of whole plants may reflect their biomass, ideally there are other traits correlated with plant size and structure that may prove predictive. Traits, such as foliar chemical content, like nitrogen (N), and morphological traits, like leaf mass area (LMA), can be predicted remotely using high-resolution leaf (Asner & Martin, 2008; Homolová et al., 2013) and canopy (Asner et al., 2016; Cawse-Nicholson et al., 2021) spectroscopy (400–2500 nm) and algorithms based on partial least squares (PLS) regression or other machine learning statistical techniques. Spectral properties can even predict chemicals not directly expressed in the spectrum, such as base cations or phosphorus (P) because these chemicals have stoichiometric relationships with chemicals that are expressed spectrally (Ustin et al., 2006). Other tree traits such as wood density can be predicted with spectroscopy, that is, traits that are not directly expressed in leaf spectra but that are instead correlated with leaf traits such as LMA (Doughty et al., 2017). Wall to wall trait maps for leaf chemistry, leaf thickness ($r^2 = 0.52$) leaf carbon

content ($r^2 = 0.70$) and maximum rates of photosynthesis ($r^2 = 0.67$) have recently been created using Sentinel-2 spectral data, soils and environmental data (Aguirre-Gutiérrez et al., 2021).

Gross primary production (GPP) and Net Primary Production (NPP) are also important fluxes to calculate, but currently are not accurately predicted for tropical forests. For instance, Cleveland et al. (2015) compared tropical NPP estimates from field-based methods, RS methods (like MODIS) and mechanistic model-based methods (like the Community Land Model -CLM). The three methods had similar estimates of NPP (i.e., $\sim 10 \text{ Mg C yr}^{-1}$), but displayed differing patterns of NPP through space and through time. The RS based methods to predict NPP made limited use of RS spectral data and relied more on climate based inputs. We are approaching the era of Surface Biology and Geology (SBG, an upcoming wall to wall hyperspectral satellite) (Cawse-Nicholson et al., 2021; Schimel & Poulter, 2022) with hopes for accurate wall to wall trait maps of tropical forests.

For this paper we focus on the extent to which plant trait data may help to improve predictions of tropical forest biomass and fluxes. We start by using a large trait database to explore whether traits can predict individual tree Diameter at Breast height (DBH), since DBH is always included in allometric equations predicting biomass, while other variables like tree height and species (to get wood density) are only sometimes included (Feldpausch et al., 2011). Next, we compare GEDI predicted biomass to field plot biomass and examine how well RS derived trait maps predict field and RS biomass. Finally, we determine the extent to which structure and traits can improve predictions of tropical forest carbon fluxes (NPP and GPP). To the best of our knowledge, this the first paper directly combining GEDI and satellite derived trait data to predict biomass. We test the following hypotheses:

- H1—Leaf spectral and trait data are correlated with (and not orthogonal to) tree diameter (DBH), an important variable for predicting biomass.
- H2—Leaf traits and environmental data will improve predictions of both field and GEDI biomass.
- H3—GEDI structure or RS trait maps will improve NPP or GPP predictions.

2. Materials and Methods

2.1. Field Leaf Trait and Spectroscopy Data

We used leaf trait and spectral data from an extensive field campaign along an elevation gradient (from 3,500 m to 220 m elevation) in the Peruvian Amazon where leaf traits for 60%–80% of basal area of trees $> 10 \text{ cm DBH}$ were measured within a well-studied 1 ha plot network from April to November 2013 (Enquist et al., 2017). In each 1 ha plot ($N = 10$ plots), we sampled the most abundant species as determined through basal area weighting (enough species generally to cover $\sim 80\%$ of the plot's basal area). For each species, we sampled the five (three in the lowlands) largest trees (based on DBH) and sampled one sun and one shade branch. On each of these branches, leaf chemistry and LMA was measured with methodology detailed in Asner et al. (2014). On five randomly selected leaves for each branch, we measured hemispherical reflectance with an ASD FieldSpec Handheld 2 with fiber optic cable, contact probe which has its own calibrated light source and a leaf clip (Analytical Spectral Devices High Intensity Contact Probe and Leaf Clip, Boulder, Colorado, USA) following (Doughty et al., 2017). We measured leaf spectroscopy (400–1,075 nm) on the same branches where the leaf traits were collected. Both LMA and Chlorophyll A had previously been shown with this data set to have a correlation with leaf spectroscopy (Doughty et al., 2017). However, we had not previously tried to compare leaf spectral data with DBH directly.

2.2. Plot Data

Aboveground biomass—We used 2,102 of 19,160 total AGB field plots that are between $+30^\circ$ and -30° latitude classified as broadleaf evergreen trees by MODIS PFT using public data (Duncanson et al., 2022) that was organized and publicly available through ORNL DAAC as an RDS (R data serialization) file. Distribution of plots are shown in Figures S1 (AGB) and S2 (residuals) in Supporting Information S1.

NPP and GPP—We also used 21, 1 ha plots where NPP and sometimes GPP were measured following the GEM protocol (Malhi et al., 2021). We focused on two regions: a Peruvian elevation transect with both NPP & GPP ($n = 10$, RAINFOR plot codes are ALP11, ALP30, SPD02, SPD01, TRU03, TRU08, TRU07, ESP01, WAY01, ACJ01 (Malhi et al., 2017)) and a Bornean logging transect with only NPP ($n = 11$ RAINFOR plot codes are DAN-04, DAN-05, LAM-01, LAM-02, MLA-01, MLA-02, SAF-01, SAF-02, SAF-03, SAF-04, SAF-05 (Riutta et al., 2018)). These plots were chosen because there are large changes in NPP/GPP across the elevation or logging gradient.

2.3. GEDI Data

We used the vertical forest structure (L2A and L2B, Version 2) and biomass (L4a) products from the GEDI instrument (R. Dubayah et al., 2020) from April 2019 to December 2022 for tropical forest regions (R. O. Dubayah et al., 2023). We used a quality filtering recipe developed in collaboration with GEDI Science Team members from University of Maryland and NASA Goddard to identify the highest quality GEDI vegetation shots (R. Dubayah et al., 2022). A data layer that this iterative local outlier detection algorithm uses to exclude data is publicly available at (R. O. Dubayah et al., 2023). For instance, some of the key data filters we applied were: include degrade flags of 0, 3, 8, 10, 13, 18, 20, 23, 28, 30, 33, 38, 40, 43, 48, 60, 63, 68, L2A and L2B quality flags = 1 (only use highest quality data), sensitivity ≥ 0.98 . With the GEDI data we used canopy height, height of median energy (HOME), and the number of canopy layers following Doughty et al. (2023).

Across all tropical forests, we created 300 by 300 m pixels containing all averaged (mean) GEDI data between 2019 and 2022. Using the centroid coordinates from each of the 2,102 plots, we found the 300 by 300 m averaged GEDI pixel that encompassed the plot. If the plot was not encompassed by the GEDI data, we searched a wider area by incrementally averaging a gradually increasing area of 1, 3, 5, and 10 pixels. In other words, if no 300 by 300 m pixel encompassed the plot, then we averaged all GEDI data an area one pixel out (4 by 4 = 1,200 by 1,200 m, 6 by 6 = 1,800 by 1,800 m, 11 by 11 = 3,300 m by 3,300 m), gradually increasing the square until it encompassed an area with GEDI data. To compare with the NPP/GPP plots we compared RS trait and GEDI data for individual footprints within a 0.03 km radius of the plot coordinates.

2.4. Remotely Sensed Leaf Trait Data

Based on a broader set of field campaigns, Aguirre-Gutiérrez et al. (2021) used Sentinel-2, climate, topographic and soil data to create remotely sensed canopy trait maps for %P = phosphorus % leaf concentration, WD = wood density g cm^{-3} , and LMA = Leaf mass area g m^{-2} .

2.5. Other Data Layers

We compared GEDI field and RS biomass estimates to several other climate and soils data sets listed below for the Amazon basin. Each data set had its own resolution, which we standardized to 0.1° by 0.1° . We used total cation exchange capacity (CEC) from soil grids (Batjes et al., 2020) in the top 0–5 cm layer in units of mmol(c) kg^{-1} . We averaged TerraClimate (Abatzoglou et al., 2018) data between 2000 and 2018 for Vapor Pressure Deficit (VPD in kPa), Mean Monthly Precipitation (mm/month), potential evapotranspiration (PET) and maximum and minimum temperature ($^\circ\text{C}$).

2.6. Statistical Analysis

We did a principal component analysis (PCA) for the tree level trait data of DBH, % of nitrogen in leaf (% N), LMA, and chl A using the matlab (Matlab, MathWorks Inc., Natick, MA, USA) function “pca”. We used the matlab function “fitlm” to fit linear models to examine the relationship between the variables, such as soils data, environmental data, leaf trait data (at 0.1° resolution) and GEDI structure data (300 m and bigger resolution), and field biomass and NPP/GPP estimates. The P values listed are for the t-statistic of the two-sided hypothesis test. We used R to create a linear model to predict the best model ranked by Akaike Information Criterion AIC and parsimony using the dredge function from the MuMIn library (Bartoń, 2009). We also used CAR package (Fox & Weisberg, 2019) and the VIF command to test for multi-collinearity between variables. To account for spatial autocorrelation, we used Simultaneous Auto-Regressive (SAR^{err}) models (Dormann et al., 2007) using the R library “spdep” (Bivand et al., 2013). We tested different neighborhood distances from 10 to 300 km and found that AIC was minimized at 80 km (Figure S3 in Supporting Information S1) and the corresponding correlogram showed reduced spatial autocorrelation (Figure S4 in Supporting Information S1). To predict leaf traits with the spectral information, we used PLS Regression (PLSR) (Geladi & Kowalski, 1986) using the PLSregress command in Matlab (Matlab, MathWorks Inc., Natick, MA, USA). To avoid over-fitting the number of latent factors we minimized the mean square error with K-fold cross validation. We use 70% of our data to calibrate our model and then the remaining 30% to test the accuracy of our model. We use adjusted r^2 , which penalizes for small sample sizes throughout the manuscript.

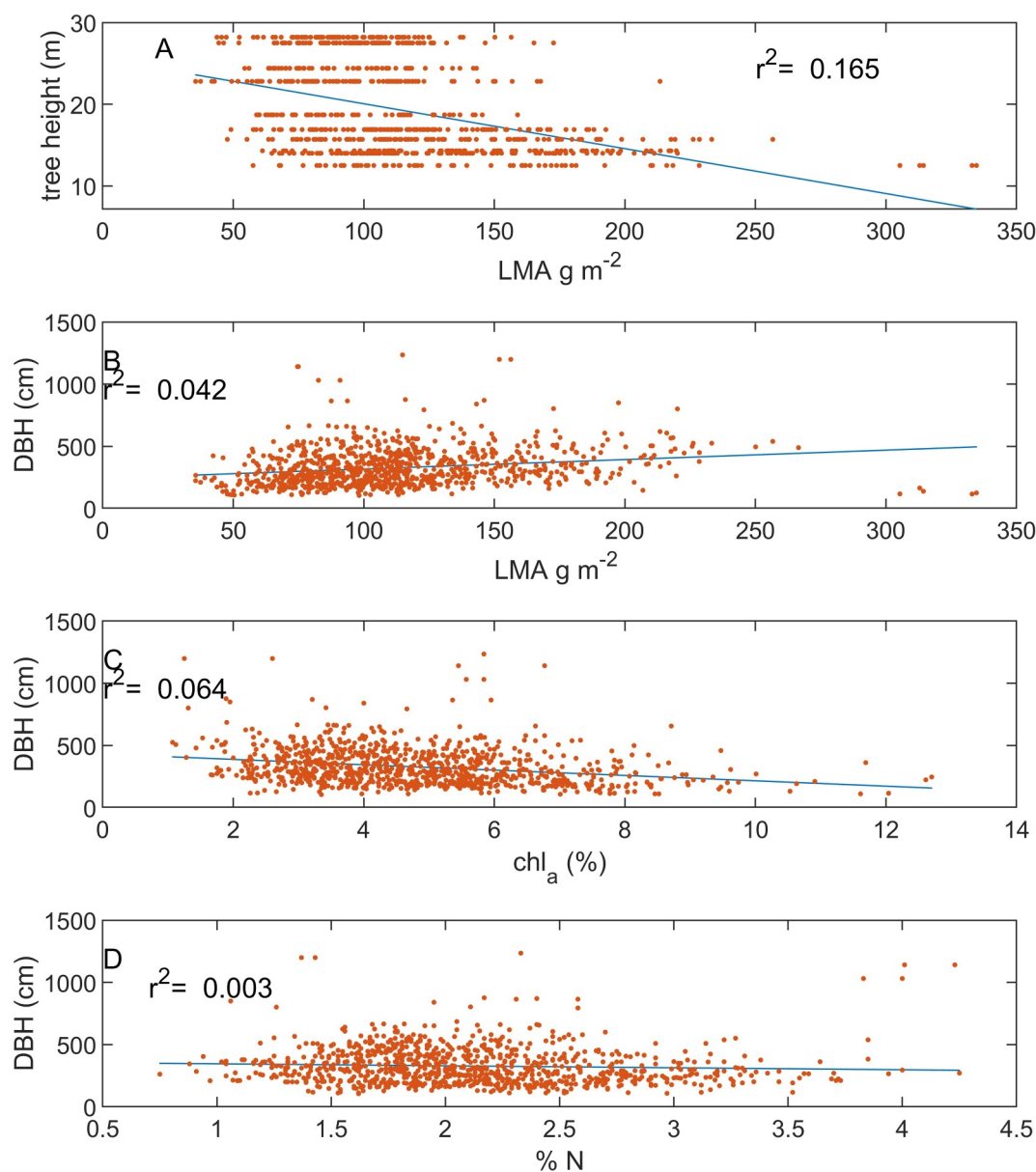


Figure 1. Individual tree height compared with leaf mass area (LMA) g m^{-2} (a), diameter at breast height compared with LMA g m^{-2} (b), % Chlorophyll A (c) and % N (d), averaged on ~ 3 branches and 5 leaves per branch.

3. Results

We examined the relationship between averaged trait values collected from cut branches and DBH of that tree for 3,695 leaves from 523 trees (Doughty et al., 2017) along a Peruvian elevation gradient and found a low correlation ($r^2 < 0.01$) between leaf chemistry (%N and %P) and DBH. However, LMA showed a significant ($P < 0.0001$) positive correlation with DBH and Chl A showed a significant ($P < 0.0001$) negative correlation but with relatively low variance explained ($r^2 = \sim 0.04$ and 0.06 respectively) (Figure 1). LMA had a significant ($P < 0.0001$) negative correlation with tree height ($r^2 = \sim 0.17$). We did a PCA for the tree level trait data of DBH, %N, LMA, and chl A and found the first principal component axis explained 94% of the variance and was dominated by DBH, while LMA dominated the second PCA axis and explained $\sim 6\%$ in the orthogonal direction (Figure S5 in Supporting Information S1). This may be why traits explain little of the variance in our data set. We then compared tree averaged leaf spectral data (400–1,075 nm) to DBH using the PLSR technique and found only a weak correlation (Figure 2, $r^2 = 0.01$). LMA is predictable with spectroscopy ($r^2 = 0.63$) and DBH is weakly

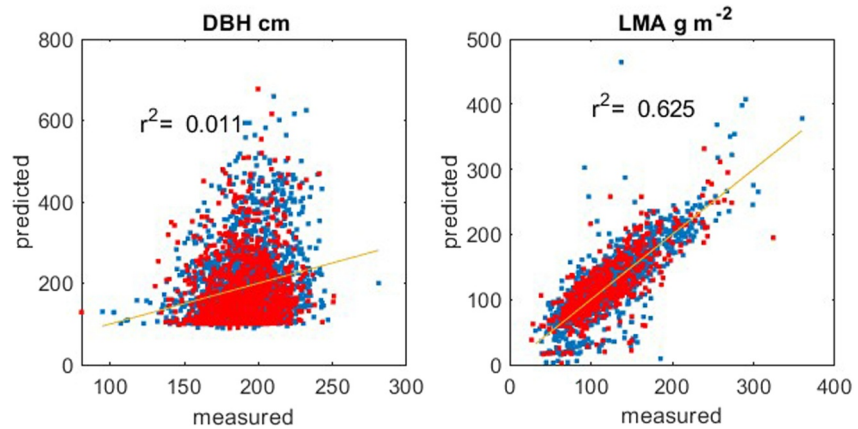


Figure 2. Leaf spectral data (400–1,075 nm) ($N = 3,695$ individual leaves) averaged on ~ 3 branches and 5 leaves per branch versus their diameter at breast height (left) or leaf mass area (right) using the partial least squares regression technique (blue is training data and red is the validation data).

predictable with LMA ($r^2 = 0.04$), and this translated into spectra being able to predict DBH with an $r^2 = 0.01$ in this data set.

We then compared predictions of GEDI biomass to 2,102, 25 m (although some plots are 1 ha) biomass plots across *all tropical forests* (not just Peru) (Figure 3). These plot data were used to create GEDI's Level 4 footprint-level AGB product using simulated waveforms from ALS collocated with field plots. In contrast, we created 300 by 300 m pixels containing all averaged (mean) GEDI data between 2019 and 2022 across all tropical forests. We acknowledge a degree of circularity in our analysis, but the comparison is different than Duncanson et al. (2022).

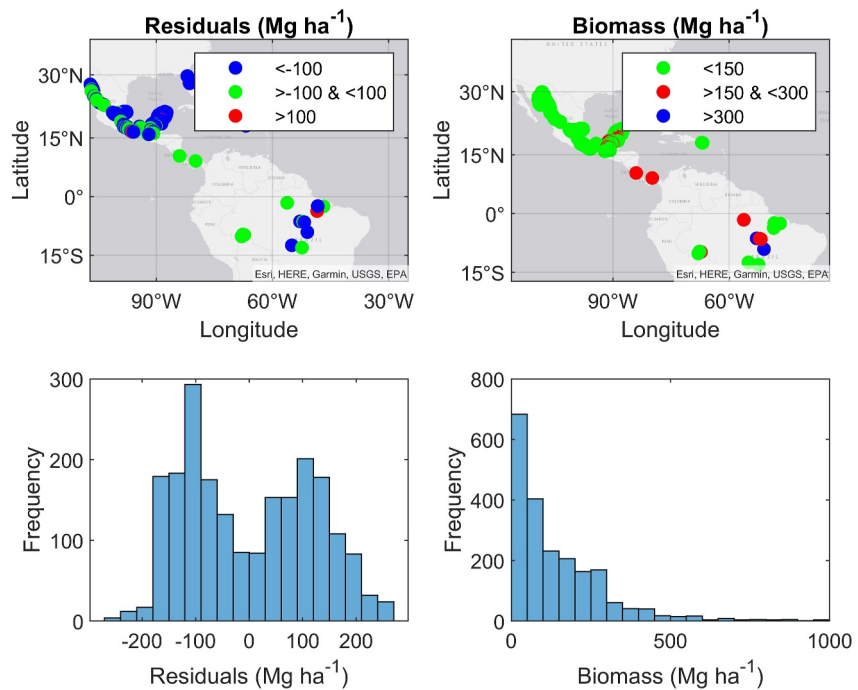


Figure 3. Global ecosystem dynamics investigation predicted biomass minus field biomass (residuals) (left) and field biomass (right) where (top) the color dots represents the value (residuals Mg ha^{-1} between 100 and $-100 =$ green, $>100 =$ red, and $<-100 =$ blue and above ground biomass $\text{Mg ha}^{-1} < 150 =$ green, between 150 and 300 = red and $>300 =$ blue). For the maps we show a subset of the data for visual clarity. The full maps are shown in Figures S1 and S2 in Supporting Information S1. On the bottom, we show a histogram of the residuals (left) and field biomass (right). All comparisons were aggregated to 300 by 300 m areas.

Because of the variable nature of GEDI data collection and the variable ISS orbital tracks, only 247 (~45%) of the plots had plot data within the 300 by 300 m pixel and ~2.5% of the plots needed an area of 3,300 m by 3,300 m. We therefore are not aligning field and GEDI data but are instead assessing regional correlations among variables of interest, thus our expected correlations will be much lower than where GEDI and field plots are geolocated and temporally aligned. We then subtracted GEDI regional averages of predicted biomass from field derived biomass (henceforth referred to as residuals) for 2,102 plots across the tropics and showed both their location, AGB, and the average difference from the GEDI predicted value (Figure 3). There are spatial patterns with the residuals with, for instance, GEDI overestimating AGB in the Yucatan Peninsula and underestimating in the Eastern Amazon. Overall, the residuals have two modes at ~-100 and 100 Mg ha⁻¹. Next, our goal is to determine whether the bias can be reduced by incorporating RS leaf traits or other external data sets.

For these 2,102 plots, there was a significant ($P < 0.0001$) negative correlation between the remotely sensed trait of LMA for both GEDI biomass ($r^2 = 0.38$) and GEDI measured forest height ($r^2 = \sim 0.43$) (Figure 4). There was a significant ($P < 0.0001$) negative correlation between remotely sensed % P and biomass and height ($r^2 = 0.31$ and $r^2 = 0.36$ respectively). However, LMA predicted field derived biomass poorly ($r^2 \sim 0.01$) and % P was not correlated with field derived biomass ($P > 0.05$). LMA was always a stronger predictor than %P, for height, RS biomass and field derived biomass. We correlated field versus remotely sensed biomass ($r^2 = \sim 0.05$) and remotely sensed tree height ($r^2 = \sim 0.03$) (note again that these are regional correlations and not exact geolocated comparisons).

We then compared LMA, %P, GEDI height and percentage one peak (an estimate of canopy stratification with 1 = more than one vertical peak in PAVD and 0 = one vertical peak in PAVD) to biomass residuals and found a negative relationship between LMA and residuals (r^2 of 0.34, $N = 66$) and a negative relationship with %P ($r^2 = 0.31$). Of GEDI structure variables, % one peak did poorly, only predicting 4% of the variance but tree height predicted biomass strongly with an r^2 of 0.74 (Figure 5). We then subset the AGB field plots for the Amazon basin ($N = 66$ of 2,102 total) to match our climate and soils data sets. We compared climate data (VPD, T_{\max} , PET) and soils data (CEC) to biomass residuals and found T_{\max} was best in predicting residuals with an r^2 of 0.79 followed by PET ($r^2 = 0.70$) and VPD ($r^2 = 0.28$) (Figure 6). We did not find a significant relationship ($P > 0.05$) between CEC and biomass residuals.

We tested for spatial autocorrelation and found that averaging around a radius of 80 km (this large radius may incorporate broader climate trends) minimized AIC (Figure S3 in Supporting Information S1) which reduced spatial autocorrelation according to the correlogram (Figure S4 in Supporting Information S1). There was some collinearity between the trait variables and structure variables ($VIF > 3$), so we removed %P and HOME and this reduced all collinearity scores to under ~1.5. To predict RS biomass, the best model by AIC included LMA, height, and % one peak, but LMA was only marginally significant (Table 1). For field biomass, the best model by AIC again included all three variables but % one peak was not significant. After controlling for spatial autocorrelation by grouping the plot data into neighborhoods of 80 km, the statistical models changed. Adding LMA (but not %P, HOME, or % one peak) significantly ($P < 0.0001$) improved field biomass predictions. Adding traits (neither LMA or P) did not significantly improve RS biomass but both % one peak and HOME did ($P < 0.0001$). We \log_{10} transformed the data (biomass, LMA and height) which improved predictions of field biomass (from r^2 of 0.03 to an r^2 of 0.16) but did not improve predictions of RS biomass. Overall, canopy height was always by far the most important predictor of AGB but adding RS LMA did improve predictions of field biomass by ~0.01 r^2 .

We then estimated NPP and GPP data with traits (LMA and % P) and structure (biomass, tree height, and % one peak). LMA showed the strongest correlation with both NPP ($r^2 = 0.38$) and GPP ($r^2 = 0.41$) (Figure 7). Tree height and % one peak were not significantly correlated with the NPP/GPP plot data. For the logging gradient in Borneo there was a significant correlation with both tree height and LMA to NPP with LMA stronger than other traits. However, when we combined the Borneo and Amazonia data sets together, only LMA remained significantly correlated with NPP (Figure 8).

4. Discussion

After controlling for spatial autocorrelation, adding RS derived LMA trait data significantly improves predictions of field measured (but not GEDI estimated) tropical forest biomass, only by a small amount (improving r^2 by ~0.01) but information criteria (AIC) suggest LMA should be added. An important caveat is that we are not

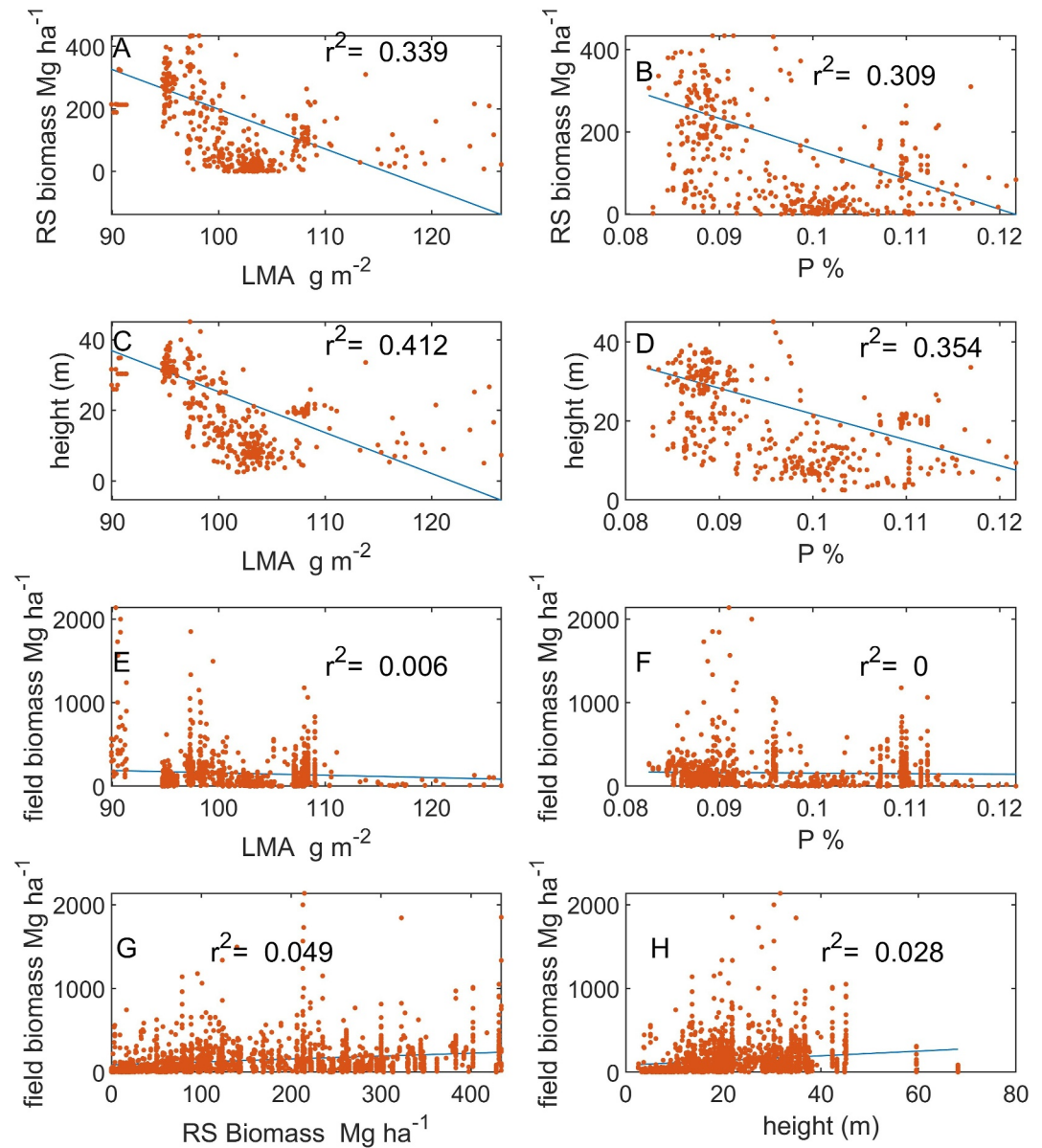


Figure 4. Leaf mass area (g m^{-2}) versus RS biomass (a) Mg ha^{-1} , tree height (c) (m), and field derived biomass (e) Mg ha^{-1} . P (%) versus RS biomass (b) Mg ha^{-1} , tree height (d) (m), and field derived biomass (f) Mg ha^{-1} . RS biomass (g) Mg ha^{-1} versus field derived biomass and (h) tree height (m) versus Mg ha^{-1} versus field derived biomass.

comparing geolocated field plot data to GEDI and trait data for the same exact area, but instead for the broader region (i.e., only 45% of the ABG plots have GEDI data within a 300 by 300 m area). This differs from the study by Duncanson et al. (2022) where airborne lidar data were used to simulate GEDI data for each plot, therefore comparing predicted GEDI structure for the same area as the field plots. Since there is much regional variation in biomass, our predictions of field measured biomass have a low r^2 ($r^2 \sim 0.03$) but were significantly improved with RS LMA data. LMA also directly predicts field biomass with an $r^2 \sim 0.01$ (Figure 4). At the individual tree scale (Figure 1), we show similar results with LMA predicting 4% of DBH variance (highly correlated with biomass) and spectral properties predicting 1% of DBH variance (Figure 2). However, predicting biomass at the canopy scale may have more success than at the leaf scale, because canopies incorporate more spectral information with higher LAI (Baret et al., 1994). Therefore, we estimate that adding RS trait data to GEDI results in a real, but very small improvement in field biomass predictability. But is this meaningful? The GEDI L4A product for tropical

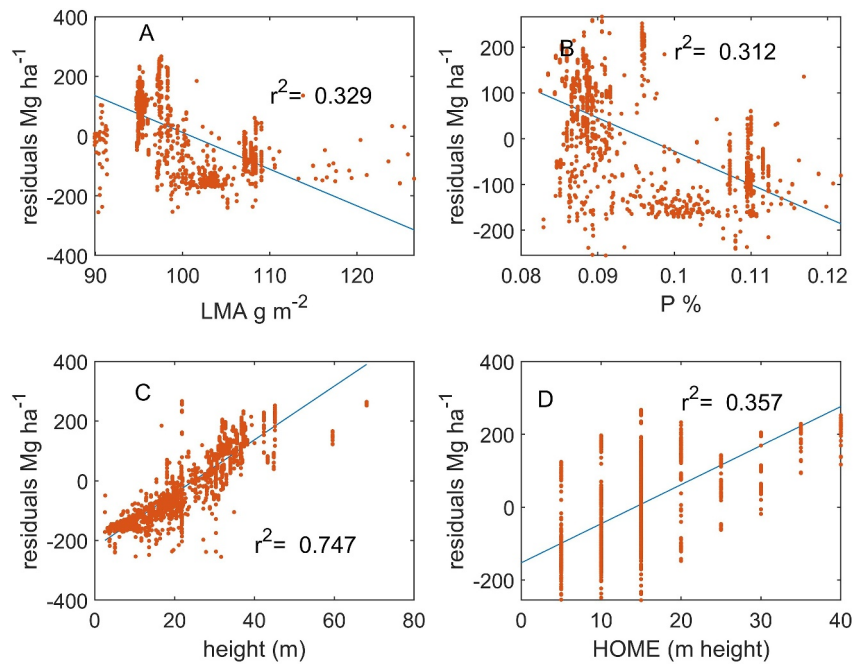


Figure 5. Biomass residuals (plot biomass minus global ecosystem dynamics investigation (GEDI) predicted biomass) versus remotely sensed leaf mass area (a), % P (b), and GEDI predicted structural variables (height (C) and HOME(d)).

forests currently has an accuracy of 0.66 r^2 (Duncanson et al., 2022), so any real improvement is welcome, if real. However, adding non-GEDI data to biomass predictions could also introduce error which could cancel out the 1% improvement.

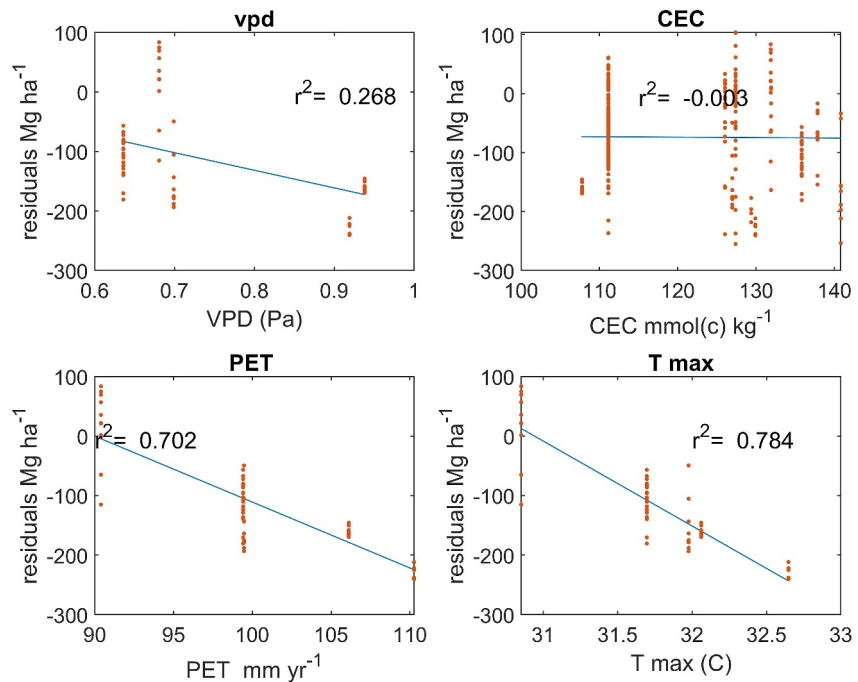


Figure 6. Biomass residuals (plot biomass minus global ecosystem dynamics investigation predicted biomass) versus soils (cation exchange capacity (CEC) and climate data (vapor pressure deficit, potential evapotranspiration, and maximum temperature (T_{max})).

Table 1
Model Results (Δ AIC and Adjusted R^2) for Field Derived Biomass, and Global Ecosystem Dynamics Investigation (GEDI) Predicted Biomass Using GEDI Measured Forest Height, GEDI Measured Maximum PAVD Height, % One Peak, and Leaf Traits of Leaf Mass Area and % P

Variables	Field derived biomass			RS biomass		
	Δ AIC	Best model	Adj r^2	Δ AIC	Best model	Adj r^2
Height, peak, P	1	Height, P, <i>PEAK</i>	0.0356	1.5	Height, peak, <i>P</i>	0.799
Height, peak, LMA		Height, peak	0.0281		Height, peak	0.799
Height, HOME, P	3	Height, P, <i>HOME</i>	0.0368	22	Height, HOME, <i>P</i>	0.795
Height, HOME, LMA	2	Height, HOME, <i>LMA</i>	0.0326	7	Height, HOME, <i>LMA</i>	0.793
Height	–		0.0272	–		0.787

Note. For Δ AIC we give the change in Δ AIC between the best model and the second-best model. The best model column gives the best model according to AIC and the variable removed (bolded and italicized) for the next best model.

Some of our results tentatively suggest that adding traits could lead to a greater improvement in AGB prediction than suggested above by reducing bias in the residuals. For instance, we found the remotely sensed trait of LMA was correlated with both GEDI biomass ($r^2 = 0.38$) and GEDI measured forest height ($r^2 = \sim 0.43$) (Figure 4). We also found both LMA (r^2 of 0.34) and %P ($r^2 = 0.31$) correlated with the biomass residuals. This suggests that traits could potentially correct for bias in current GEDI predictions, which could be more useful than a 0.01 improvement in r^2 . However, because the leaf traits maps use predictors of soils and climate data in addition to Sentinel 2 spectral data, the improvements to biomass prediction may be due to the influence of the underlying climate variables as shown in Figure 6. LMA and %P correlated more with RS AGB than field AGB possibly for this reason as well. We focused on using trait data in tropical forests because remotely sensed species detection is difficult (Feret & Asner, 2013; Mulatu et al., 2017), but similar approaches could potentially be used in lower diversity temperate and boreal forests as well. There is optimism for future improvements in predictability because our leaf spectral data only extends through 1,075 nm, and there is likely important spectral information at longer wavelengths (e.g., in the shortwave infrared). The current RS trait maps (Aguirre-Gutiérrez et al., 2021) use a few Sentinel 2 spectral bands but future satellites like SBG (Cawse-Nicholson et al., 2021; Schimel & Poulter, 2022) or the Plankton, Aerosol, Cloud, ocean Ecosystem mission (Gorman et al., 2019) will have improved or wall to wall hyperspectral data and therefore future, more accurate trait maps may improve biomass estimates by a greater amount or reduce uncertainties.

Our strongest (non-GEDI) predictor of biomass residuals was T_{\max} with an r^2 of 0.79, but we note that this is based on a much smaller Amazon only data set ($N = 66$) (Figure 6). The negative correlation suggests that GEDI underpredicts biomass in regions where VPD or T_{\max} is on average higher. Stressful temperature or aridity may reduce tree biomass and height from their maximum potential or select for smaller species with more conservative strategies. This result is supported by literature showing higher temperatures reducing tropical forest growth rates (Clark et al., 2003). Soil cation concentration was not a strong predictor of biomass residuals in our data set which is surprising because soil cation concentrations are the primary driver of floristic variation for Amazonian trees (Tuomisto et al., 2019) with climate being of secondary importance.

In a previous paper, we had hypothesized that forest stratification (% one peak or the number of single stratum forests as a percentage of total) might improve biomass predictions better than a simple metric like rh50 (Doughty et al., 2023) because in that paper, % one peak predicted biomass better than tree height. Ecological theory suggests that a stratified forest with more large emergent trees is indicative of an older forest (Halle et al., 1980), which generally has higher biomass and carbon content. However, in our study, % one peak was a fairly poor predictor of the residuals explaining only 4% of the variance. This compares with other traits that predicted more variance such as 75% with tree height, 16% with rh50 and 36% with HOME. When we added % one peak to our overall model it did not improve the AIC, and therefore seems a poor predictor of biomass across tropical forests. We also found a high correlation between GEDI height and biomass residuals (Figure 5c), which may be due to the transformation (log or square root) of biomass in GEDI L4A models such that error increases as biomass/height increases. Further, a recent paper found that GEDI accurately predict redwood tree heights but still underestimates AGB because tree height may not be an accurate predictor for high biomass forests

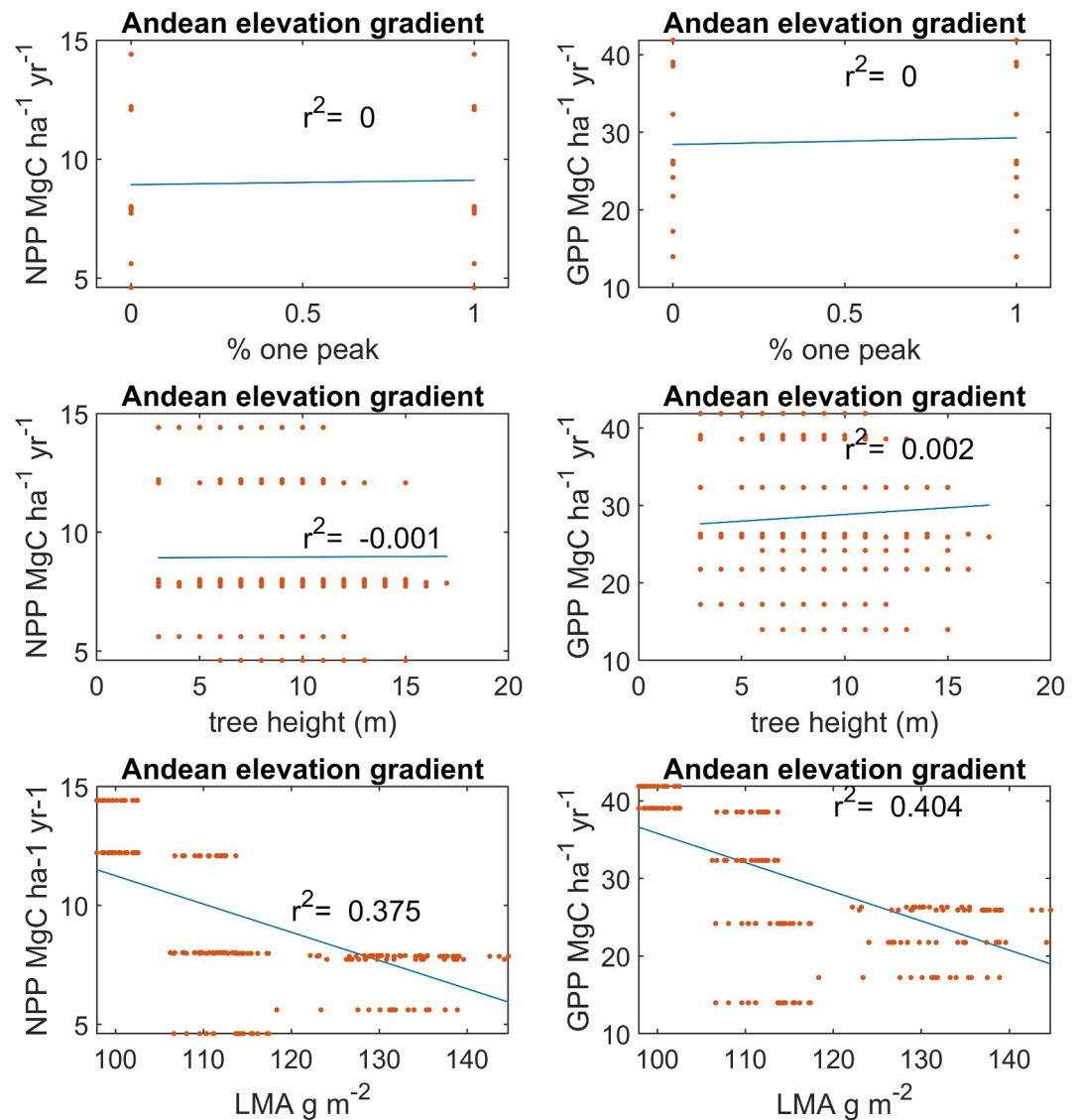


Figure 7. Net Primary Production (left) and Gross primary production (right) data from South America compared to % one peak (top) (an estimate of canopy stratification with 1 = more than one vertical peak in PAVD and 0 = one vertical peak in PAVD), global ecosystem dynamics investigation (GED) calculated tree height (middle), and remote sensed leaf mass area (bottom). GEDI data are from the nearest 0.03° pixel.

(Sillett et al., 2024). Moving forward, terrestrial lidar can expand our understanding of tree structure and possibly create improved biomass estimates beyond DBH (Stovall & Shugart, 2018).

Remotely sensed MODIS NPP and GPP is a commonly used input to many global models (Zhang et al., 2012) but previous studies have found that MODIS NPP does not match ground based estimates of NPP seasonality and therefore, there is a need for improved remote sensed NPP estimates (Cleveland et al., 2015). Our results (Figures 7 and 8) suggest that adding trait maps to predictions of GPP and NPP could potentially improve accuracy, but GEDI structure metrics did not improve predictability. For instance, remotely sensed LMA predicted GPP ($r^2 = 0.4$) and NPP ($r^2 = 0.35$) better than GEDI height in an Andean elevation gradient (Figure 7). When we combined both data sets, only LMA continued to predict NPP (Figure 8). However, although we used the biggest NPP and GPP data set in the tropics, our sample size ($N = 21$) was small. More ground based NPP/GPP networks are necessary for validation before we would have confidence in this result.

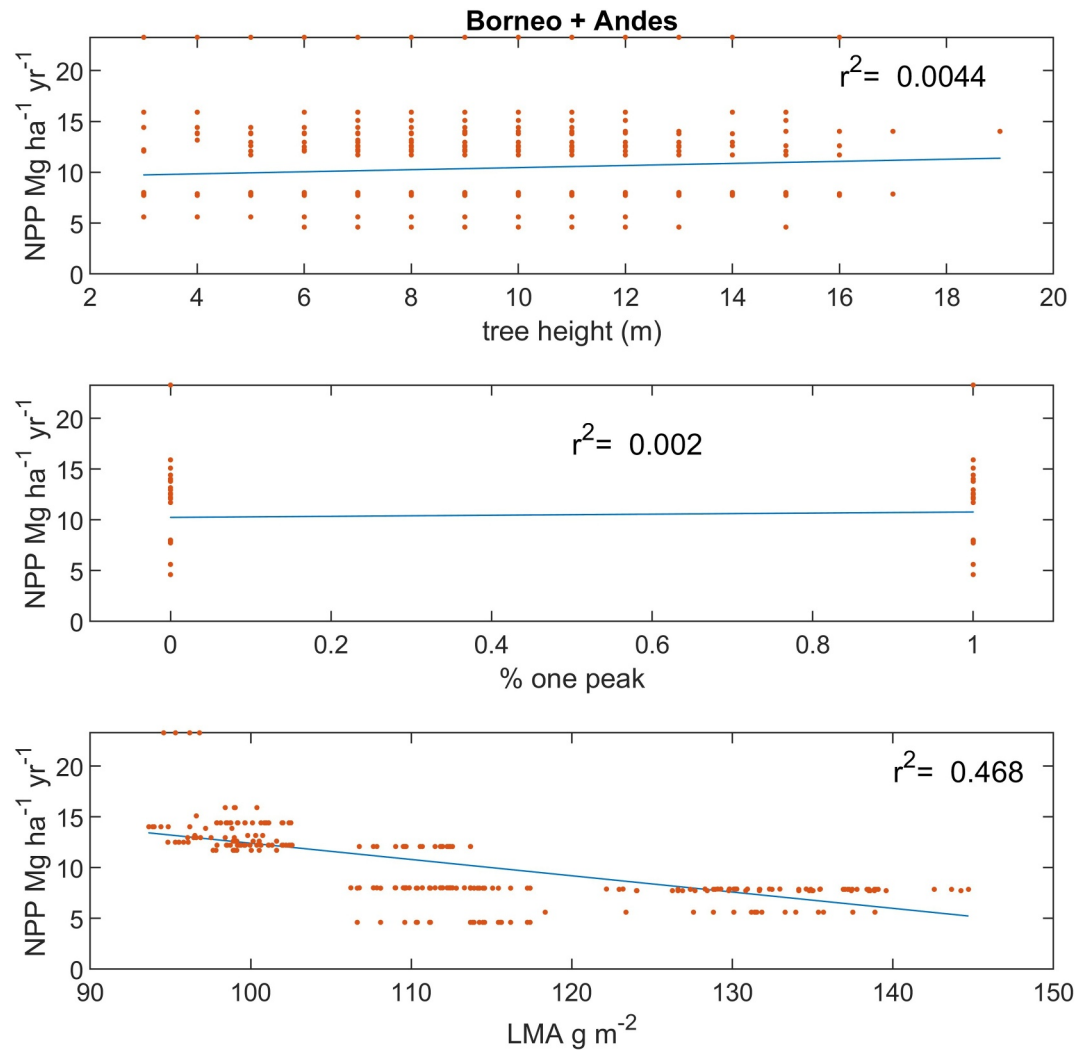


Figure 8. Net Primary Production data from Borneo and South America compared to global ecosystem dynamics investigation calculated tree height (top), % one peak (middle) (an estimate of canopy stratification with 1 = more than one vertical peak in PAVD and 0 = one vertical peak in PAVD) and remote sensed leaf mass area (bottom).

Overall, we show several lines of evidence (tree DBH vs. leaf traits, tree DBH vs. spectroscopy, RS traits vs. field biomass, RS traits vs. field NPP/GPP) that traits can slightly improve estimates of tropical forest biomass and fluxes and possibly may be further improved in the future with data from new satellite missions like SBG. Other potential improvements in remote biomass estimates might come from integrating dynamic vegetation models that have trait data with GEDI observations (Ma et al., 2023).

Data Availability Statement

Description of the Type(s) of data and/or software. Data—Data and its descriptions to create all figures and tables in this paper are available (Doughty, 2024). Software—All code and its descriptions to create all figures and tables in this paper are available (Doughty, 2024).

Acknowledgments

This work was funded by a NASA GEDI Grant 80NSSC21K0191. It was also made possible due to the data collection efforts of many people from the GEM network (Malhi et al., 2021) and the people who collected data for the biomass plots from Duncanson et al. (2022).

References

- Abatzoglou, J. T., Dobrowski, S. Z., Parks, S. A., & Hegewisch, K. C. (2018). TerraClimate, a high-resolution global dataset of monthly climate and climatic water balance from 1958–2015. *Scientific Data*, 5(1), 170191. <https://doi.org/10.1038/sdata.2017.191>
- Aguirre-Gutiérrez, J., Rifai, S., Shenkin, A., Oliveras, I., Bentley, L. P., Svátek, M., et al. (2021). Pantropical modelling of canopy functional traits using Sentinel-2 remote sensing data. *Remote Sensing of Environment*, 252, 112122. <https://doi.org/10.1016/j.rse.2020.112122>
- Asner, G. P., Knapp, D. E., Anderson, C. B., Martin, R. E., & Vaughn, N. (2016). Large-scale climatic and geophysical controls on the leaf economics spectrum. *Proceedings of the National Academy of Sciences of the United States of America*. <https://doi.org/10.1073/pnas.1604863113>
- Asner, G. P., & Martin, R. E. (2008). Spectral and chemical analysis of tropical forests: Scaling from leaf to canopy levels. *Remote Sensing of Environment*, 112(10), 3958–3970. <https://doi.org/10.1016/j.rse.2008.07.003>
- Asner, G. P., Martin, R. E., Carranza-Jimenez, L., Sinca, F., Tupayachi, R., Anderson, C. B., & Martinez, P. (2014). Functional and biological diversity of foliar spectra in tree canopies throughout the Andes to Amazon region. *New Phytologist*, 204(1), 127–139. <https://doi.org/10.1111/nph.12895>
- Asner, G. P., & Mascaro, J. (2014). Mapping tropical forest carbon: Calibrating plot estimates to a simple LiDAR metric. *Remote Sensing of Environment*, 140, 614–624. <https://doi.org/10.1016/j.rse.2013.09.023>
- Avitabile, V., Herold, M., Heuvelink, G. B. M., Lewis, S. L., Phillips, O. L., Asner, G. P., et al. (2016). An integrated pan-tropical biomass map using multiple reference datasets. *Global Change Biology*, 22(4), 1406–1420. <https://doi.org/10.1111/gcb.13139>
- Baccini, A., Goetz, S. J., Walker, W. S., Laporte, N. T., Sun, M., Sulla-Menashe, D., et al. (2012). Estimated carbon dioxide emissions from tropical deforestation improved by carbon-density maps. *Nature Climate Change*, 2(3), 182–185. <https://doi.org/10.1038/nclimate1354>
- Baret, F., Vanderbilt, V. C., Steven, M. D., & Jacquemoud, S. (1994). Use of spectral analogy to evaluate canopy reflectance sensitivity to leaf optical properties. *Remote Sensing of Environment*, 48(2), 253–260. [https://doi.org/10.1016/0034-4257\(94\)90146-5](https://doi.org/10.1016/0034-4257(94)90146-5)
- Bartoni, K. (2009). MuMIn: Multi-model inference. R Package Version 0.12.2.
- Batjes, N. H., Ribeiro, E., & van Oostrum, A. (2020). Standardised soil profile data to support global mapping and modelling (WoSIS snapshot 2019). *Earth System Science Data*, 12(1), 299–320. <https://doi.org/10.5194/essd-12-299-2020>
- Bivand, R., Hauke, J., & Kossowski, T. (2013). Computing the Jacobian in Gaussian spatial autoregressive models: An illustrated comparison of available methods. *Geographical Analysis*, 45(2), 150–179. <https://doi.org/10.1111/gean.12008>
- Cawse-Nicholson, K., Townsend, P. A., Schimel, D., Assiri, A. M., Blake, P. L., Buongiorno, M. F., et al. (2021). NASA's surface biology and geology designated observable: A perspective on surface imaging algorithms. *Remote Sensing of Environment*, 257, 112349. <https://doi.org/10.1016/j.rse.2021.112349>
- Clark, D. A., Piper, S. C., Keeling, C. D., & Clark, D. B. (2003). Tropical rain forest tree growth and atmospheric carbon dynamics linked to interannual temperature variation during 1984–2000. *Proceedings of the National Academy of Sciences of the United States of America*, 100(10), 5852–5857. <https://doi.org/10.1073/pnas.0935903100>
- Cleveland, C. C., Taylor, P., Chadwick, K. D., Dahlin, K., Doughty, C. E., Malhi, Y., et al. (2015). A comparison of plot-based satellite and Earth system model estimates of tropical forest net primary production. *Global Biogeochemical Cycles*, 29(5), 626–644. <https://doi.org/10.1002/2014GB005022>
- Díaz, S., Kattge, J., Cornelissen, J. H. C., Wright, I. J., Lavorel, S., Dray, S., et al. (2016). The global spectrum of plant form and function. *Nature*, 529(7585), 167–171. <https://doi.org/10.1038/nature16489>
- Dormann, C. F., McPherson, J. M., Araújo, M. B., Bivand, R., Bolliger, J., Carl, G., et al. (2007). Methods to account for spatial autocorrelation in the analysis of species distributional data: A review. *Ecography*, 30(5), 609–628. <https://doi.org/10.1111/j.2007.0906-7590.05171.x>
- Doughty, C. (2024). Satellite-derived trait data slightly improves tropical forest biomass, NPP, and GPP predictions [Dataset]. *Dryad*. <https://doi.org/10.5061/dryad.ttdz08m5n>
- Doughty, C. E., Gaillard, C., Burns, P., Keany, J. M., Abraham, A. J., Malhi, Y., et al. (2023). Tropical forests are mainly unstratified especially in Amazonia and regions with lower fertility or higher temperatures. *Environmental Research: Ecology*, 2(3), 35002. <https://doi.org/10.1088/2752-664X/ace723>
- Doughty, C. E., Santos-Andrade, P. E., Goldsmith, G. R., Blonder, B., Shenkin, A., Bentley, L. P., et al. (2017). Can leaf spectroscopy predict leaf and forest traits along a Peruvian tropical forest elevation gradient? *Journal of Geophysical Research: Biogeosciences*, 122(11), 2952–2965. <https://doi.org/10.1002/2017JG003883>
- Dubayah, R., Armston, J., Healey, S. P., Bruening, J. M., Patterson, P. L., Kellner, J. R., et al. (2022). GEDI launches a new era of biomass inference from space. *Environmental Research Letters*, 17(9), 95001. <https://doi.org/10.1088/1748-9326/ac8694>
- Dubayah, R., Blair, J. B., Goetz, S., Fatoyinbo, L., Hansen, M., Healey, S., et al. (2020). The Global Ecosystem Dynamics Investigation: High-resolution laser ranging of the Earth's forests and topography. *Science of Remote Sensing*, 1, 100002. <https://doi.org/10.1016/j.srs.2020.100002>
- Dubayah, R. O., Armston, J., Healey, S. P., Yang, Z., Patterson, P. L., Saarela, S., et al. (2023). *GEDI LAB gridded aboveground biomass density, version 2.1*. ORNL Distributed Active Archive Center. <https://doi.org/10.3334/ORNLDAA/2299>
- Duncanson, L., Kellner, J. R., Armston, J., Dubayah, R., Minor, D. M., Hancock, S., et al. (2022). Aboveground biomass density models for NASA's Global Ecosystem Dynamics Investigation (GEDI) lidar mission. *Remote Sensing of Environment*, 270, 112845. <https://doi.org/10.1016/j.rse.2021.112845>
- Enquist, B. J., Bentley, L. P., Shenkin, A., Maitner, B., Savage, V., Michaletz, S., et al. (2017). Assessing trait-based scaling theory in tropical forests spanning a broad temperature gradient. *Global Ecology and Biogeography*, 26(12), 1357–1373. <https://doi.org/10.1111/gcb.12645>
- Feldpausch, T. R., Banin, L., Phillips, O. L., Baker, T. R., Lewis, S. L., Quesada, C. A., et al. (2011). Height-diameter allometry of tropical forest trees. *Biogeosciences*, 8(5), 1081–1106. <https://doi.org/10.5194/bg-8-1081-2011>
- Feret, J.-B., & Asner, G. P. (2013). Tree species discrimination in tropical forests using airborne imaging spectroscopy. *IEEE Transactions on Geoscience and Remote Sensing*, 51(1), 73–84. <https://doi.org/10.1109/TGRS.2012.2199323>
- Fox, J., & Weisberg, S. (2019). An R companion to applied regression.
- Geladi, P., & Kowalski, B. R. (1986). Partial least-squares regression: A tutorial. *Analytica Chimica Acta*, 185, 1–17. [https://doi.org/10.1016/0003-2670\(86\)80028-9](https://doi.org/10.1016/0003-2670(86)80028-9)
- Goetz, S. J., Hansen, M., Houghton, R. A., Walker, W., Laporte, N., & Busch, J. (2015). Measurement and monitoring needs, capabilities and potential for addressing reduced emissions from deforestation and forest degradation under REDD+. *Environmental Research Letters*, 10(12), 123001. <https://doi.org/10.1088/1748-9326/10/12/123001>
- Gorman, E. T., Kubalak, D. A., Patel, D., Dress, A., Mott, D. B., Meister, G., & Werdell, P. J. (2019). The NASA Plankton, Aerosol, Cloud, ocean Ecosystem (PACE) mission: An emerging era of global, hyperspectral Earth system remote sensing. *Proceedings of SPIE*, 11151, 111510G. <https://doi.org/10.1117/12.2537146>

- Halle, F., Oldeman, R., & Tomlinson, P. (1980). *Tropical trees and forests: An architectural analysis*. Springer.
- Hancock, S., Armston, J., Hofton, M., Sun, X., Tang, H., Duncanson, L. L., et al. (2019). The GEDI simulator: A large-footprint waveform lidar simulator for calibration and validation of spaceborne missions. *Earth and Space Science*, 6(2), 294–310. <https://doi.org/10.1029/2018EA000506>
- Homolová, L., Malenovský, Z., Clevers, J. G. P. W., García-Santos, G., & Schaepman, M. E. (2013). Review of optical-based remote sensing for plant trait mapping. *Ecological Complexity*, 15, 1–16. <https://doi.org/10.1016/j.ecocom.2013.06.003>
- Ma, L., Hurr, G., Tang, H., Lamb, R., Lister, A., Chini, L., et al. (2023). Spatial heterogeneity of global forest aboveground carbon stocks and fluxes constrained by spaceborne lidar data and mechanistic modeling. *Global Change Biology*, 29(12), 3378–3394. <https://doi.org/10.1111/gcb.16682>
- Malhi, Y., Girardin, C., Metcalfe, D. B., Doughty, C. E., Aragão, L. E. O. C., Rifai, S. W., et al. (2021). The Global Ecosystems Monitoring network: Monitoring ecosystem productivity and carbon cycling across the tropics. *Biological Conservation*, 253, 108889. <https://doi.org/10.1016/j.biocon.2020.108889>
- Malhi, Y., Girardin, C. A. J., Goldsmith, G. R., Doughty, C. E., Salinas, N., Metcalfe, D. B., et al. (2017). The variation of productivity and its allocation along a tropical elevation gradient: A whole carbon budget perspective. *New Phytologist*, 214(3), 1019–1032. <https://doi.org/10.1111/nph.14189>
- Mitchard, E. T. A., Feldpausch, T. R., Brienen, R. J. W., Lopez-Gonzalez, G., Monteagudo, A., Baker, T. R., et al. (2014). Markedly divergent estimates of Amazon forest carbon density from ground plots and satellites. *Global Ecology and Biogeography*, 23(8), 935–946. <https://doi.org/10.1111/geb.12168>
- Mitchard, E. T. A., Saatchi, S. S., Baccini, A., Asner, G. P., Goetz, S. J., Harris, N. L., & Brown, S. (2013). Uncertainty in the spatial distribution of tropical forest biomass: A comparison of pan-tropical maps. *Carbon Balance and Management*, 8(1), 10. <https://doi.org/10.1186/1750-0680-8-10>
- Mulatu, K. A., Mora, B., Kooistra, L., & Herold, M. (2017). Biodiversity monitoring in changing tropical forests: A review of approaches and new opportunities. *Remote Sensing*, 9(10), 1059. <https://doi.org/10.3390/rs9101059>
- Réjou-Méchain, M., Mortier, F., Bastin, J.-F., Cornu, G., Barbier, N., Bayol, N., et al. (2021). Unveiling African rainforest composition and vulnerability to global change. *Nature*, 593(7857), 90–94. <https://doi.org/10.1038/s41586-021-03483-6>
- Riutta, T., Malhi, Y., Kho, L. K., Marthews, T. R., Huaraca Huasco, W., Khoo, M., et al. (2018). Logging disturbance shifts net primary productivity and its allocation in Bornean tropical forests. *Global Change Biology*, 24(7), 2913–2928. <https://doi.org/10.1111/gcb.14068>
- Saatchi, S. S., Harris, N. L., Brown, S., Lefsky, M., Mitchard, E. T. A., Salas, W., et al. (2011). Benchmark map of forest carbon stocks in tropical regions across three continents. *Proceedings of the National Academy of Sciences of the United States of America*, 108(24), 9899–9904. <https://doi.org/10.1073/pnas.1019576108>
- Schimmel, D. S., & Poulter, B. (2022). The Earth in living color - NASA's surface biology and geology designated observable. In *2022 IEEE aerospace conference (AERO)* (pp. 1–6). <https://doi.org/10.1109/AERO53065.2022.9843640>
- Sillett, S. C., Graham, M. E., Montague, J. P., Antoine, M. E., & Koch, G. W. (2024). Ground-based calibration for remote sensing of biomass in the tallest forests. *Forest Ecology and Management*, 561, 121879. <https://doi.org/10.1016/j.foreco.2024.121879>
- Stovall, A. E. L., & Shugart, H. H. (2018). Improved biomass calibration and validation with terrestrial LiDAR: Implications for future LiDAR and SAR missions. *IEEE Journal of Selected Topics in Applied Earth Observations and Remote Sensing*, 11(10), 3527–3537. <https://doi.org/10.1109/JSTARS.2018.2803110>
- ter SteegePitman, H. N. C. A. H., Pitman, N. C. A., Phillips, O. L., Chave, J., Sabatier, D., Duque, A., et al. (2006). Continental-scale patterns of canopy tree composition and function across Amazonia. *Nature*, 443(7110), 444–447. <https://doi.org/10.1038/nature05134>
- Tuomisto, H., Van doninck, J., Ruokolainen, K., Moulatlet, G. M., Figueiredo, F. O. G., Sirén, A., et al. (2019). Discovering floristic and geoeological gradients across Amazonia. *Journal of Biogeography*, 46(8), 1734–1748. <https://doi.org/10.1111/jbi.13627>
- Ustin, S. L., Asner, G. P., Gamon, J. A., Fred Huemmrich, K., Jacquemoud, S., Schaepman, M., & Zarco-Tejada, P. (2006). Retrieval of quantitative and qualitative information about plant pigment systems from high resolution spectroscopy. In *International geoscience and remote sensing symposium (IGARSS)*. <https://doi.org/10.1109/IGARSS.2006.517>
- Zhang, F., Chen, J. M., Chen, J., Gough, C. M., Martin, T. A., & Dragoni, D. (2012). Evaluating spatial and temporal patterns of MODIS GPP over the conterminous U.S. against flux measurements and a process model. *Remote Sensing of Environment*, 124, 717–729. <https://doi.org/10.1016/j.rse.2012.06.023>